Electric-field control of the chiral magnetism of multiferroic $MnWO_4$ as seen via polarized neutron diffraction

T. Finger,[1] D. Senff,[1] K. Schmalzl,[2] W. Schmidt,[2] L. P. Regnault,[3] P. Becker,[4] L. Bohatý,[4] and M. Braden[1,*]

[1]*II. Physikalisches Institut, Universität zu Köln, Zülpicher Str. 77, D-50937 Köln, Germany*

[2]*Institut für Festkörperforschung, Forschungszentrum Jülich GmbH, JCNS at ILL, 38042 Grenoble Cedex 9, France*

[3]*Institut Nanosciences et Cryogénie, CEA-Grenoble, DRFMC-SPSMS-MDN, 38054 Grenoble Cedex 9, France*

[4]*Institut für Kristallographie, Universität zu Köln, Zülpicher Str. 49b, D-50674 Köln, Germany*

(Received 5 November 2009; revised manuscript received 9 December 2009; published 18 February 2010)

The chiral components in the magnetic order in multiferroic $MnWO_4$ have been studied by neutron diffraction using spherical polarization analysis as a function of temperature and of external electric field. We show that sufficiently close to the ferroelectric transition at $T=12.3$ K it is possible to switch the chiral component by applying moderate electric fields at constant temperature. Full hysteresis cycles can be observed which indicate strong pinning of the magnetic order. $MnWO_4$, furthermore, exhibits a magnetoelectric memory effect across heating into the paramagnetic and paraelectric phase.

DOI: 10.1103/PhysRevB.81.054430 PACS number(s): 75.80.+q, 61.05.fm, 75.25.−j, 75.60.Ch

I. INTRODUCTION

Magnetoelectric materials allow one to tune the electric polarization by an external magnetic field and to tune magnetic polarization by an electric field.[1–3] In particular, the control of magnetic order by an electric field has a strong application potential in the context of data storage but in spite of strong efforts no suitable materials have been discovered so far.[2,3]

Concerning the recently discovered multiferroic transition-metal oxides[3,4] it has been well established that the ferroelectric polarization can be modified by an external magnetic field.[4,5] Using polarized neutron scattering in $TbMnO_3$,[5] $LiCu_2O_2$,[6] and in $MnWO_4$,[7] it has also been shown that the chiral component of the magnetic order can be poled by an electric field when cooling through the ferroelectric transition. However, in general there have been only very few reports on a change in a magnetic order induced by applying an electric field at constant temperature.[8–12] For $MnWO_4$ it was shown that by varying the electric field one may induce a hysteresis in the ferroelectric polarization[13] and in the second harmonic generation.[14] However, the direct observation of the electric-field-induced switching of the chiral magnetism at constant temperature has not been reported so far in the spiral multiferroics although this effect is most important in view of applications.[3,4]

In most of the recently discovered multiferroics, the ferroelectric polarization can be explained by the inverse Dzyaloshinski-Moriya effect,[15,16] where the induced electric polarization of a single pair of spins S_i, S_j separated by a distance vector $\mathbf{r}_{i,j}$ is given by[15]

$$\mathbf{P}_{FE} \propto \mathbf{r_{ij}} \times (\mathbf{S_i} \times \mathbf{S_j}). \quad (1)$$

The required noncollinear magnetic structure may arise from strong frustration. Since in addition the interaction, Eq. (1), is only a second-order effect, the ferroelectric polarization is rather small in these materials. In the $REMnO_3$ (Refs. 4 and 17) series and in $MnWO_4$ (Refs. 18–20) the electric polarization is about two to three orders of magnitude smaller than that in a standard ferroelectric perovskite such as $BaTiO_3$, hindering the observation of electric-field-induced effects in the magnetic structure. Nevertheless, we show in this work that it is possible in these chiral multiferroics to switch the magnetic order by the application of a moderate electric field at constant temperature.

The magnetic order in $MnWO_4$ (space group $P2/c$, $a=4.835$ Å, $b=5.762$ Å, $c=4.992$ Å, and $\beta=91.08°$) has been determined by neutron diffraction.[21] Upon cooling, $MnWO_4$ first undergoes a transition into an incommensurate magnetic phase labeled AF3 with propagation vector $\mathbf{q}_{ic}=(-0.214, 0.5, 0.457)$ and collinear moments aligned in the a-c plane, $T_{AF3}=13.2$ K. At the second transition, $T_{AF2}=12.3$ K, the b component develops giving rise to a still incommensurate but noncollinear phase, AF2. At the transition AF3 → AF2 the ferroelectric polarization develops, as independently discovered by three groups.[18–20] At further cooling, the magnetic order transforms into a commensurate collinear AF1 state with $\mathbf{q}_c=(-0.25, 0.5, 0.5)$, $T_{AF1}=7.0$ K.

II. EXPERIMENTAL

The polarized neutron-diffraction experiments were performed on the IN12 cold triple-axis spectrometer at the Institut Laue-Langevin using either Helmholtz coils or the zero-field Cryopad for polarization analysis. An untwined single crystal[18] was set in a (0,1,0), (−0.214, 0, 0.457) scattering plane. The dimensions of the crystal were $4\times4\times21$ mm^3 and it was fully covered by the beam. The electric field was applied along the b direction by setting an external voltage of up to 3500 V thus yielding electric fields of up to $E=875$ V/mm. On a structural Bragg reflection we have determined the flipping ratio of our polarization setup to 40 and 35 in the two experimental runs.

III. POLING OF THE CHIRAL STATE AND ITS MEMORY EFFECT

The unpolarized neutron-scattering intensity is given by the square of the magnetic structure factor, $\mathbf{M}_\perp(\mathbf{Q}) = r_0 N^{1/2} \Sigma_j [\mathbf{M}_j - (\mathbf{Q}\cdot\mathbf{M}_j)\frac{\mathbf{Q}}{Q^2}] e^{i\mathbf{Q}\cdot\mathbf{R_j}}$, where $r_0=5.4fm$,

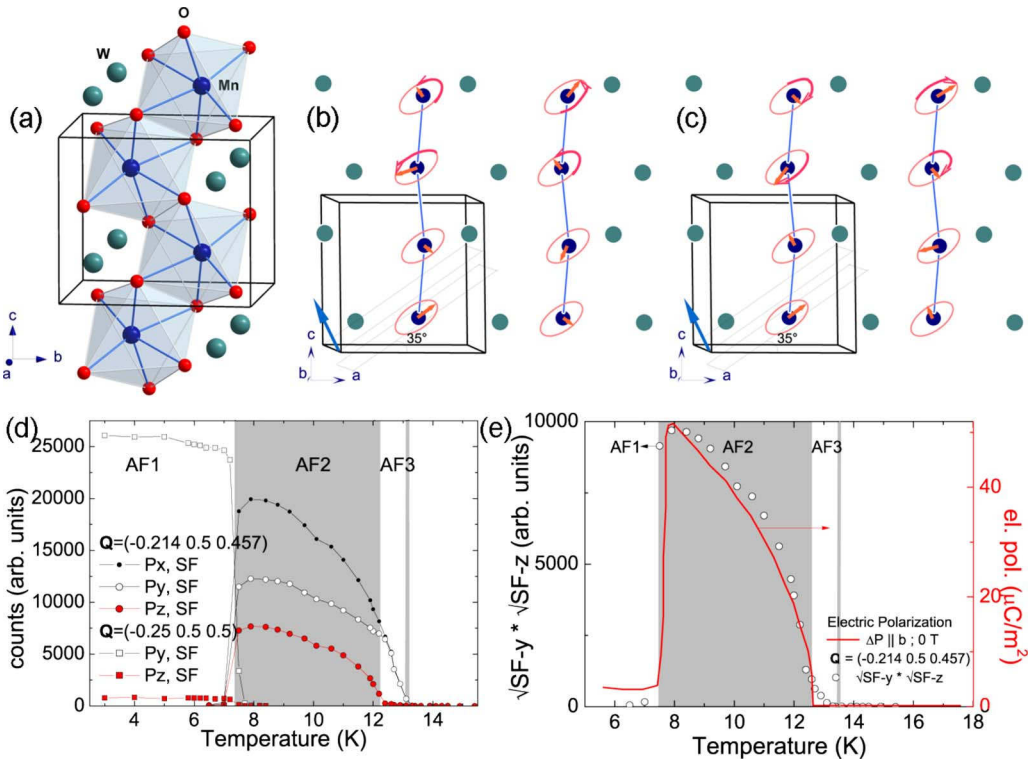

FIG. 1. (Color online) (a) Crystal and [(b) and (c)] magnetic structure in $MnWO_4$; (b) and (c) show the two opposite chiral arrangements; the arrow on the bottom left of the schematic unit cell indicates the direction of the propagation vector, which is almost perpendicular to the easy axis. Note that the magnetic moments at the two Mn sites within a single unit cell are not related through the propagation vector but by the magnetic symmetry; therefore we do not add a clockwise or anticlockwise arrow. [(d) and (e)] Temperature dependence of magnetic scattering at q_{ic} and q_c studied with polarized neutron diffraction. The experiment was performed in the (0,1,0), (−0.214,0,0.457) scattering plane; part (d) shows the magnetic scattering polarized parallel to the easy axis and that parallel to b and part (e) the product of the magnetic components along these two directions, $\sqrt{\sigma_{yy}^{\uparrow\downarrow}}\cdot\sqrt{\sigma_{zz}^{\uparrow\downarrow}}$, which scales well with the ferroelectric polarization (Ref. 19).

Q denotes the wave vector, and the sum runs over the atoms in the cell with complex moment $\mathbf{M}_j$ at position $\mathbf{R}_j$. We use the common Cartesian coordinate system with **x** along **Q**, **y** in the scattering plane but perpendicular to **Q**, and **z** as vertical. The polarization analysis[22] adds additional selection rules: in the spin-flip (SF) scattering the contributing magnetization must be perpendicular to the neutron polarization. By measuring the three SF channels for $\mathbf{P}\|\mathbf{x}=(-0.214,0.5,0.457)=\mathbf{Q}$, $\mathbf{P}\|\mathbf{y}$, and $\mathbf{P}\|\mathbf{z}$, we may thus follow the components as a function of temperature, see Fig. 1. In the AF3 phase the magnetic moment aligns along an easy axis, $\mathbf{e}_{\mathbf{easy}}$, in the a-c plane nearly perpendicular to the propagation vector $\mathbf{q}_{ic}$ (the angle amounts to 83°). Therefore, almost all elastic magnetic scattering is found in the $\mathbf{P}\|\mathbf{y}$ channel and no magnetic signal is found for $\mathbf{P}\|\mathbf{z}$. The latter channel directly senses the b component and becomes finite upon the phase transition into the AF2 phase. The ferroelectric polarization[18–20] only crudely scales with the b component, see Fig. 1(d). At the transition into the AF1 phase the b component measured in the $\mathbf{P}\|\mathbf{z}$ channel disappears as does the ferroelectric polarization.[18–20]

The three-dimensional polarization analysis using Cryopad allows one to determine the full polarization tensor by analyzing the outgoing and incoming polarization independently.[22] $\sigma_{ij}^{\downarrow\uparrow}$ denotes the intensity in the channel with the outgoing polarization along j when the incoming polarization is set along i with the arrows indicating the directions of polarizations. The magnetic scattering can be decomposed into the $M_y(\mathbf{Q})M_y^*(\mathbf{Q})$ and $M_z(\mathbf{Q})M_z^*(\mathbf{Q})$ contributions and the chiral term, $\mathbf{M}_{ch}(\mathbf{Q})=i\{\mathbf{M}_\perp(\mathbf{Q})\times\mathbf{M}_\perp^*(\mathbf{Q})\}$, which rotates the neutron polarization toward the scattering vector, and which possesses only a finite x component $M_{ch}(\mathbf{Q})$.

The chiral term is determined in three spherical polarization channels. In comparison to the total magnetic scattering it is measured in the xx channel as $\sigma_{xx}^{\downarrow\uparrow}=[M_y(\mathbf{Q})M_y^*(\mathbf{Q})+M_z(\mathbf{Q})M_z^*(\mathbf{Q})]-M_{ch}(\mathbf{Q})$ and $\sigma_{xx}^{\uparrow\downarrow}=[M_y(\mathbf{Q})M_y^*(\mathbf{Q})+M_z(\mathbf{Q})M_z^*(\mathbf{Q})]+M_{ch}(\mathbf{Q})$ by

$$r_{chir}=\frac{M_{ch}(\mathbf{Q})}{M_y(\mathbf{Q})M_y^*(\mathbf{Q})+M_z(\mathbf{Q})M_z^*(\mathbf{Q})}=\frac{\sigma_{xx}^{\uparrow\downarrow}-\sigma_{xx}^{\downarrow\uparrow}}{\sigma_{xx}^{\uparrow\downarrow}+\sigma_{xx}^{\downarrow\uparrow}}. \quad (2)$$

Alternatively, the chiral contribution is measured at the nondiagonal components of the polarization tensor

$$r_{chir}=\frac{\sigma_{yx}^{\uparrow\downarrow}-\sigma_{yx}^{\uparrow\uparrow}}{\sigma_{yx}^{\uparrow\downarrow}+\sigma_{yx}^{\uparrow\uparrow}}=\frac{\sigma_{yx}^{\downarrow\downarrow}-\sigma_{yx}^{\downarrow\uparrow}}{\sigma_{yx}^{\downarrow\uparrow}+\sigma_{yx}^{\downarrow\downarrow}} \quad (3)$$

in the yx and similarly in the zx channels. In Eqs. (2) and (3) we may neglect any nuclear contribution as the Bragg-peaks studied are purely magnetic. Polarized neutron scattering directly probes the chiral term.

If the magnetic order in the sample crystal is a perfect transverse spiral with the spiral plane perpendicular to the

propagation vector $\mathbf{q_{ic}}$ parallel to $\mathbf{Q}$, the spin-flip scattering $\sigma_{xx}^{\downarrow\uparrow}$ or $\sigma_{xx}^{\uparrow\downarrow}$ is finite for only one incident polarization, since $M_{ch}(\mathbf{Q})$ and $M_y(\mathbf{Q})M_y^*(\mathbf{Q})+M_z(\mathbf{Q})M_z^*(\mathbf{Q})$ are of the same absolute size yielding $r_{chir}=\pm 1$.[23] If the geometrical condition that $\mathbf{Q}$ is perpendicular to the chiral plane, is no longer fulfilled the chiral contribution to the scattering r_{chir} is reduced even for the ideal monodomain transverse spiral. In order to detect a strong chiral term one needs to choose an appropriate scattering vector. Furthermore, with a real crystal it is necessary to align the chiral domains, which in the multiferroics can be obtained by applying an electric field.[5–7] After cooling the sample to $T=7.7$ K applying an electric field of 3500 V/4mm we have measured the full three-dimensional polarization matrix at $\mathbf{Q}=(-0.214,0.5,0.457)$ and $(-0.214,1.5,0.457)$ as well as at the (0,2,0) structural Bragg reflections. At the first magnetic reflection the chiral contribution is dominant: the obtained chiral ratio amounts to 80.8%. We also find strong contributions in the yx and zx channels, which, according to Eq. (3) indicate $r_{chir}=80.3\%$ and 80.6%, respectively, in perfect agreement with the value found by the diagonal term. The chiral contributions are much weaker at the second reflection since the large b component of the scattering vector suppresses the scattering strength of this magnetic component compared to that along $\mathbf{e_{easy}}$. For $\mathbf{Q}=(-0.214,1.5,0.457)$, we only find chiral contributions of 31.0%, 32.9%, and 32.3% in the xx, yx, and zx channels, respectively. In the refinements of the magnetic structure[21] it was not possible to determine the phase between the $\mathbf{e_{easy}}$ and b components of the ordered magnetic moment, which however determines the collinear or chiral nature of the magnetic structure and thereby the strength of the multiferroic coupling, see Eq. (1). Analyzing the full spherical polarization tensor we may confirm that the phase between the two components is close to 90° corresponding to a chiral arrangement. Therefore, we may confirm that Eq. (1) fully explains the occurrence and the direction of the ferroelectric polarization in $MnWO_4$.[24] Indeed, the product of the magnetic components along the easy direction and along b measured by $\sqrt{\sigma_{yy}^{\uparrow\downarrow}}\cdot\sqrt{\sigma_{zz}^{\uparrow\downarrow}}$ scales very well with the temperature dependence of the ferroelectric polarization, see Fig. 1(e). From the depolarization of the beam polarized initially along y or z we further estimate that with the applied electric field one obtains a nearly perfect alignment of the chiral component; only ~5% of the sample remain in the opposed chiral state.

In various heating-cooling cycles we found that $MnWO_4$ remembers its chiral state even after heating into the paramagnetic and paraelectric phase. The memory and hysteresis behavior of $MnWO_4$ appears to be very complex and is very difficult to be fully reproduced as it seems to depend on the cooling velocity across the magnetic transitions.[25] To illustrate the complex memory effect in $MnWO_4$ we show in Fig. 2 two sets of thermal cycles, Figs. 2(a)–2(d) and Figs. 2(e)–2(h), which were separated by heating to high temperature (~295 K). First we cooled the crystal in −3500 V obtaining the almost perfectly aligned chiral component which we label arrangement A, see Figs. 1(b) and 1(c). After heating to 15 K, i.e., into the paramagnetic and paraelectric state, and recooling in zero electric field we find the identical chiral component, see Fig. 2(b). Heating once more and recooling in the opposed electric field allows one to fully switch the chiral alignment to arrangement B. Finally another heating to 15 K with successive zero-field cooling results in the same arrangement A although the preceding +3500 V experiment yielded arrangement B. This clearly documents that the crystal remembers the alignment of the chiral contribution even in the paraelectric and paramagnetic phase. Apparently the first cooling in electric field results in a preference of the crystal for arrangement A, which is not erased by forcing the sample with the opposed electric field into arrangement B. After heating the sample to room temperature we performed a similar series of thermal cycling starting with the positive electric field. Again one may pole the sample into both arrangements, although the alignment is less perfect. But now the state B is the one observed in the zero-field-cooling cycles independently of the preceding direction of the electric field. One can force the sample crystal into a preferred chiral arrangement depending on the first cooling from high temperature. This finding resembles the previously reported memory effect across the paraelectric collinear magnetic phase AF1 (Ref. 26) and the magnetic-field-driven reversibility.[14] The fact that the preference is robust against heating deeply into the paramagnetic state, however, seems to exclude the given interpretation[26] in terms of ferroelectric embryos. It appears more likely that the hysteresis and preference arise from multiferroic domain pinning by defects or by extrinsic distortions, see below.

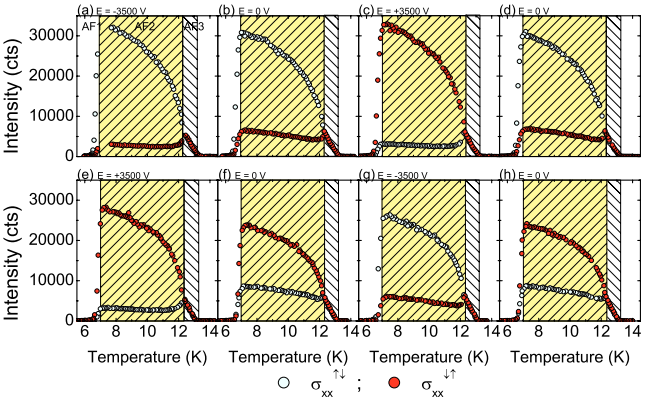

FIG. 2. (Color online) Temperature dependence of the magnetic scattering in the $\sigma_{xx}^{\uparrow\downarrow}$ and $\sigma_{xx}^{\downarrow\uparrow}$ channels measured upon cooling the $MnWO_4$ crystal with and without electric field. Note that the intensity in the two xx spin-flip channels reflect the volumes of the two chiral arrangements shown in Figs. 1(b) and 1(c). [(a)–(d)] After first cooling in negative electric field the cycles were successively recorded by cooling in −3500, 0, +3500, and 0 V. [(e)–(h)] Before starting the second run of thermal cycles, we heated the sample up to room temperature and then measured the cooling cycles in +3500, 0, −3500, and 0 V.

IV. ELECTRIC-FIELD CONTROL OF CHIRAL MAGNETISM

In two sets of experiments we studied the possibility to control the chiral arrangement by varying the electric field at constant temperature. After cooling the sample in negative

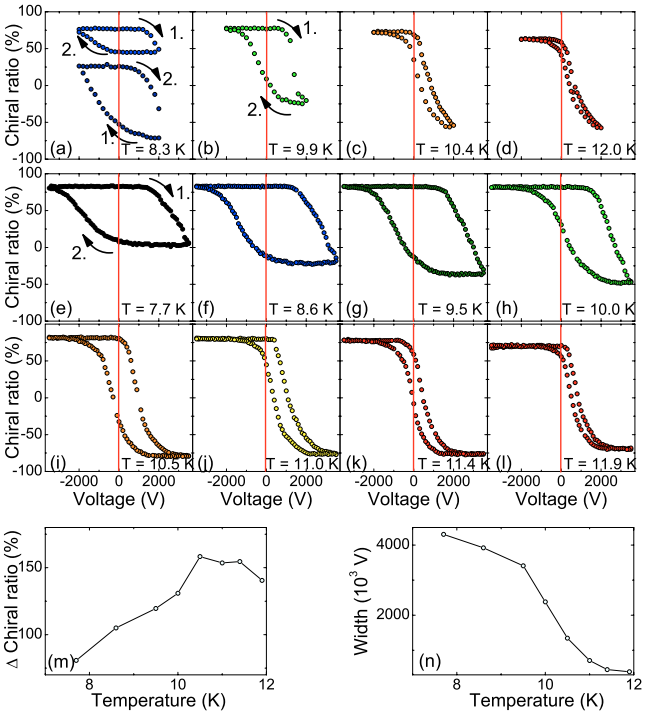

FIG. 3. (Color online) Hysteresis curves of the chiral ratio as a function of external electric field at constant temperature; [(a)–(d)] hysteresis cycles were recorded after electric-field cooling in $E=-2000$ V [only the lower cycle in (a)] was recorded after cooling in +2000 V. [(e)–(l)] Hysteresis curves were recorded after cooling in −3500 V; (m) and (n) present the electric-field-induced difference in the chiral ratio and the width of the hysteresis measured at the middle value as function of temperature, respectively.

voltage we have measured a hysteresis cycle of the chiral ratio versus electric field at $T=8.3$ K. When fully reducing the voltage to zero the chiral ratio is unchanged; the voltage may even be inverted and increased to +1000 V without any significant change in the chiral component documenting the effective pinning of the magnetism in $MnWO_4$. But further increase in the voltage significantly reduces the chiral ratio. Upon cycling the voltage back to the initial negative value the chiral ratio rapidly approaches the starting value. A quite different hysteresis curve is observed when the cycle is recorded after cooling with a positive voltage from about 15 K, following cooling from room temperature in negative voltage, see Fig. 3(a). The initial chiral ratio is of opposite sign but of the same size as that obtained upon cooling with the negative voltage, $r_{chir\text{-}initial}=-81\%$, but when lowering the voltage the chiral term immediately diminishes and even fully changes sign when the voltage is increased in the negative direction. When driving the voltage from −2000 V back to zero the weaker positive chiral ratio remains unchanged and only partially recovers the initial value for increasing the voltage to +2000 V. Other hysteresis cycles at higher temperatures were obtained after field cooling at −2000 V from 15 K. When approaching the AF2–AF3 transition, larger effects are induced in these cycles and the width of the hysteresis becomes smaller but all hysteresis curves remain asymmetric indicating the preferred chiral arrangement. At $T=12.0$ K we can induce a complete inversion of the chiral arrangement through the inversion of the electric field. There is no indication for an altered magnetic structure; the switching of the chiral terms corresponds to an inversion of the chiral domains. Such electric-field control of magnetism forms the basis of the data-storage application of multiferroic materials.

In the following run we recorded several hysteresis cycles after cooling from high temperature in negative voltage attaining $U=-3500$ V at low temperatures, see Figs. 3(e)–3(l). The same asymmetric hysteresis curves are obtained and again it is possible to fully control the chiral component by the electric field. Just the width of the hysteresis clearly increases with the larger maximum electric field. At $T=10.5$ K nearly identical hysteresis cycles were obtained at the four **Q** positions $(\pm 0.214, 0.5, \mp 0.457)$ and $(\pm 0.214, -0.5, \mp 0.457)$. With increasing temperature the height of the hysteresis passes a maximum as the control is facilitated closer to the magnetic transition whereas the size of the chiral component diminishes, see Fig. 3(m). The width of the asymmetric hysteresis continuously decreases upon approaching the paraelectric phase as one may expect due to a weaker pinning, see Fig. 3(n). However, note that the coercitive fields are significantly higher in our large sample than those reported in Refs. 13 and 14.

The hysteresis cycles shown in Fig. 3 offer a view on the processes pinning the magnetism in the multiferroic material. Well below T_{AF2}, the chiral domains are efficiently pinned and an inversion cannot be obtained in our large crystal with the moderate electric fields. Close to the transition the full magnetic inversion is possible but the hysteresis cycle remains very asymmetric. Even after passing into the paramagnetic phase the sample crystal exhibits a pronounced memory for the chiral domains forced in preceding field-cooling cycles. It must be left to future experiments to study the exact temperature (apparently well above 30 K) which is needed in the heating cycle in order to erase this memory. The strong pinning and asymmetry of the chiral domains must be based on strong magnetoelectroelastic coupling or on some ferroelectric fatigue. If the ferroelectric polarization is purely electronic in origin the associated pinning force should be negligible, whereas a ferroelectric polarization due to ionic displacements can posses an intrinsic pinning capability. The pinning of the chiral may also arise from higher harmonic components which we indeed observe in $MnWO_4$. The second-order harmonics of the magnetic modulation studied at $\mathbf{Q}=(-0.428, 1.0, 0.914)$ shows magnetic and sizeable nuclear components. These second-order modulations, furthermore, are closely coupled, as we find clear nuclear-magnetic interference. The magnetism in $MnWO_4$ is thus not only associated with an anharmonic magnetic contribution but also with a structural modulation which can be pinned by defects or by an extrinsic distortion. When cooling an as-grown crystal, a certain multiferroic domain structure is written, in which domains and defects fit to each other. In this virgin or any following cooling, defects may move or even be generated thereby forming the memory. In succeeding cooling cycles the identical chiral domain structure forms, see Figs. 2(b), 2(d), 2(f), and 2(h) unless another domain structure can be enforced, see Figs. 2(c) and 2(g). The latter effect is possible in multiferroic $MnWO_4$ by the application of the electric field.

V. CONCLUSIONS

In conclusion we have studied the impact of an external electric field on the magnetic structure in $MnWO_4$. The electric poling of the chiral terms exhibits a memory effect even when heating into the paramagnetic and paraelectric phase, most likely due to pinning of multiferroic domains by defects or by extrinsic distortions. Most importantly, we show that one may control the chiral magnetism by varying the electric field at constant temperature in the multiferroic phase. It is possible to observe full multiferroic hysteresis curves.

Note added in proof: Recently we learned that a qualitatively similar hysteresis curve in $MnWO_4$ was reported (See Ref. 27).

ACKNOWLEDGMENT

This work was supported by the Deutsche Forschungsgemeinschaft through the Sonderforschungsbereich 608.

*braden@ph2.uni-koeln.de

[1] W. Eerenstein, N. D. Mathur, and J. F. Scott, Nature (London) **442**, 759 (2006).
[2] G. A. Smolenskiĭ and I. E. Chapuis, Sov. Phys. Usp. **25**, 475 (1982).
[3] S.-W. Cheong and M. Mostovoy, Nature Mater. **6**, 13 (2007).
[4] T. Kimura, T. Goto, H. Shintani, K. Ishizaka, T. Arima, and Y. Tokura, Nature (London) **426**, 55 (2003).
[5] Y. Yamasaki, H. Sagayama, T. Goto, M. Matsuura, K. Hirota, T. Arima, and Y. Tokura, Phys. Rev. Lett. **98**, 147204 (2007).
[6] S. Seki, Y. Yamasaki, M. Soda, M. Matsuura, K. Hirota, and Y. Tokura, Phys. Rev. Lett. **100**, 127201 (2008).
[7] H. Sagayama, K. Taniguchi, N. Abe, T. H. Arima, M. Soda, M. Matsuura, and K. Hirota, Phys. Rev. B **77**, 220407(R) (2008).
[8] E. Ascher, H. Rieder, H. Schmid, and H. Stössel, J. Appl. Phys. **37**, 1404 (1966).
[9] T. Lottermoser, T. Lonkai, U. Amann, D. Hohlwein, J. Ihringer, and M. Fiebig, Nature (London) **430**, 541 (2004).
[10] Y. Bodenthin, U. Staub, M. Garcia-Fernandez, M. Janoschek, J. Schlappa, E. I. Golovenchits, V. A. Sanina, and S. G. Lushnikov, Phys. Rev. Lett. **100**, 027201 (2008).
[11] T. Zhao, A. Scholl, F. Zavaliche, K. Lee, M. Barry, A. Doran, M. P. Cruz, Y. H. Chu, C. Ederer, N. A. Spaldin, R. R. Das, D. M. Kim, S. H. Baek, C. B. Eom, and R. Ramesh, Nature Mater. **5**, 823 (2006).
[12] D. Lebeugle, D. Colson, A. Forget, M. Viret, A. M. Bataille, and A. Goukasov, Phys. Rev. Lett. **100**, 227602 (2008).
[13] B. Kundys, C. Simon, and C. Martin, Phys. Rev. B **77**, 172402 (2008).
[14] D. Meier, M. Maringer, T. Lottermoser, P. Becker, L. Bohaty, and M. Fiebig, Phys. Rev. Lett. **102**, 107202 (2009).
[15] H. Katsura, N. Nagaosa, and A. V. Balatsky, Phys. Rev. Lett. **95**, 057205 (2005); M. Mostovoy, *ibid.* **96**, 067601 (2006); I. A. Sergienko and E. Dagotto, Phys. Rev. B **73**, 094434 (2006).
[16] T. Kimura, G. Lawes, T. Goto, Y. Tokura, and A. P. Ramirez, Phys. Rev. B **71**, 224425 (2005).
[17] T. Goto, T. Kimura, G. Lawes, A. P. Ramirez, and Y. Tokura, Phys. Rev. Lett. **92**, 257201 (2004).
[18] O. Heyer, N. Hollmann, I. Klassen, S. Jodlauk, L. Bohatý, P. Becker, J. A. Mydosh, T. Lorenz, and D. Khomskii, J. Phys.: Condens. Matter **18**, L471 (2006).
[19] K. Taniguchi, N. Abe, T. Takenobu, Y. Iwasa, and T. Arima, Phys. Rev. Lett. **97**, 097203 (2006).
[20] A. H. Arkenbout, T. T. M. Palstra, T. Siegrist, and T. Kimura, Phys. Rev. B **74**, 184431 (2006).
[21] G. Lautenschläger, H. Weitzel, T. Vogt, R. Hock, A. Bohm, M. Bonnet, and H. Fuess, Phys. Rev. B **48**, 6087 (1993).
[22] T. Chatterji, *Neutron Scattering from Magnetic Materials* (Elsevier, Amsterdam, 2006).
[23] It is not possible to assign a chirality (or handedness) to a cycloid since the propagation vector and the spiral plane are parallel. Therefore, we refer to the chiral component $\mathbf{M}_{ch}$ in order to access the chiral domains.
[24] In the case of $MnWO_4$ it is not sufficient to analyze the nearest-neighbor spins in order to explain the ferroelectric polarization along b since the spin-wave dispersion shows that this interaction is not dominating. However summing Eq. (1) over all spin pairs the spiral arrangement with $\mathbf{e}_{\mathbf{easy}}$ and b components also generates a ferroelectric polarization along b.
[25] The cooling velocity was difficult to control due to the delicate balance between exchange gas and applied field.
[26] K. Taniguchi, N. Abe, S. Ohtani, and T. Arima, Phys. Rev. Lett. **102**, 147201 (2009).
[27] A. Poole, P. J. Brown, and A. S. Wills, J. Phys.: Conf. Ser. **145**, 012074 (2009).